Geo-Mar Lett (2006) 26: 213–224
DOI 10.1007/s00367-006-0023-5

ORIGINAL

S. L. Yang · T. Kvalstad · A. Solheim · C. F. Forsberg

Parameter studies of sediments in the Storegga Slide region

Received: 15 June 2005 / Accepted: 29 May 2006 / Published online: 8 July 2006

Abstract Based on classification tests, oedometer tests, fall-cone tests and triaxial tests, physical and mechanical properties of sediments in the Storegga Slide region were analysed to assess parameter interrelationships. The data show good relationships between a number of physical and mechanical parameters. Goodness of fit between compression index and various physical parameters can be improved by multiple regression analysis. The interclay void ratio and liquidity index correlate well with the undrained shear strength of clay. Sediments with higher water content, liquid limit, activity, interclay void ratio, plasticity index and liquidity index showed higher compression index and/or lower undrained shear strength. Some relationships between parameters were tested by using data from two other sites south of the Storegga Slide. A better understanding of properties of sediments in regions such as that of the Storegga Slide can be obtained through this approach.

Introduction

Submarine slides form a frequent phenomenon of the world's continental margins, including the glacier-fed, clay-dominated margins of high latitudes (Mienert et al. 2003). Hence, a better understanding of the behaviour and geotechnical properties of various clay-rich deposits is important for an improved study of submarine slides. Commonly in geological investigations, index physical properties are measured on a routine basis whereas other geotechnical properties, such as compressibility and undrained shear strength, are more rarely assessed, particularly at greater depths. Thus, if index properties such as water contents, Atterberg limits and grain-size distributions can be used in a more quantitative estimation of the geotechnical behaviour of clay-rich sediments, then this would be very useful for investigations of the stability of clays.

The Storegga Slide offshore mid-Norway occurred 8,200 years ago (Haflidason et al. 2005). Because Norway's second largest gas field, Ormen Lange, is located in the slide scar, the area has been intensively investigated to ensure safe field development (Solheim et al. 2005). In addition, several other large projects have been carried out in the region, both by industry and academic institutions, as well as by the Ocean Drilling Program (Eldholm et al. 1987; Mienert 2004). Whereas gravity corers and piston corers are common sampling tools in many geological investigations, a number of deep geological and geotechnical boreholes have been drilled in the Storegga Slide area. The boreholes range from 20 to 450 m in depth, and most were also logged using wireline geophysical tools. Although sampling was relatively sparse and samples were taken at irregular intervals through the drilled sections, all important lithological units within the slide-prone part of the sedimentary column were accounted for. Various geotechnical tests were performed on this material, and a detailed database of geotechnical, geological and geophysical parameters has been established, making an investigation of parameter interrelationships readily possible within this geological setting.

The present study focuses on data from classification analyses (grain-size distribution, Atterberg limits, water content), oedometer tests, and measurements of undrained shear strength by means of fall-cone apparatus, pocket penetrometer and anisotropic compression triaxial tests. Relationships between these parameters were assessed in terms of simple and multiple regression analyses. The objectives of the study are twofold: (1) to derive relationships which could be used to estimate the geotechnical properties and behaviour of such sediments; and (2) to obtain a better understanding of the behaviour of sediments involved in the Storegga Slide.

S. L. Yang (✉) · T. Kvalstad · A. Solheim · C. F. Forsberg
International Centre for Geohazards,
Norwegian Geotechnical Institute,
0806 Oslo, Norway
e-mail: shaoli.yang@ngi.no
Tel.: +47-22023182
Fax: +47-22230448

Study site and geological setting

Data from 28 boreholes were used in this study (Fig. 1, Table 1). Most of the sites are located in the Storegga Slide scar but some, including the ODP sites, are found further to the north on the Vøring Plateau (Fig. 1). In addition to the sites along the Mid-Norwegian margin, comparative data (NGI 2002) from the North Sea petroleum fields Troll East (TE) and Sleipner B (SB), which are located south of the Storegga Slide area, were used to check some of the correlations obtained for the main study area.

The Storegga Slide morphology has been extensively described in several recent papers (e.g. Haflidason et al. 2004, 2005; Berg et al. 2005). The sediments in this area were deposited in response to glacial–interglacial variations and consist primarily of two main classes. Thus, periods of peak glaciations, with ice extending to the shelf break, are characterised by tills on the continental shelf and

Table 1 Boreholes in the study area

Project	Site no.	Stress history
Seabed	Helland Hansen East, Helland Hansen SW, Nyk High, Gjallar Ridge	Normally consolidated
ODP	642, 643, 644	Normally consolidated
Ormen Lange	17, 18, 19, 20, 22, 27, 28, 31, 99, PL1-7, PL_02, OB1, OB2, NF	Highly overconsolidated samples at sites 17, 18, partly at sites 22, 27, 99, 31, OB1, OB2, PL1-7, PL_02
Other	MD99	Partly overconsolidated

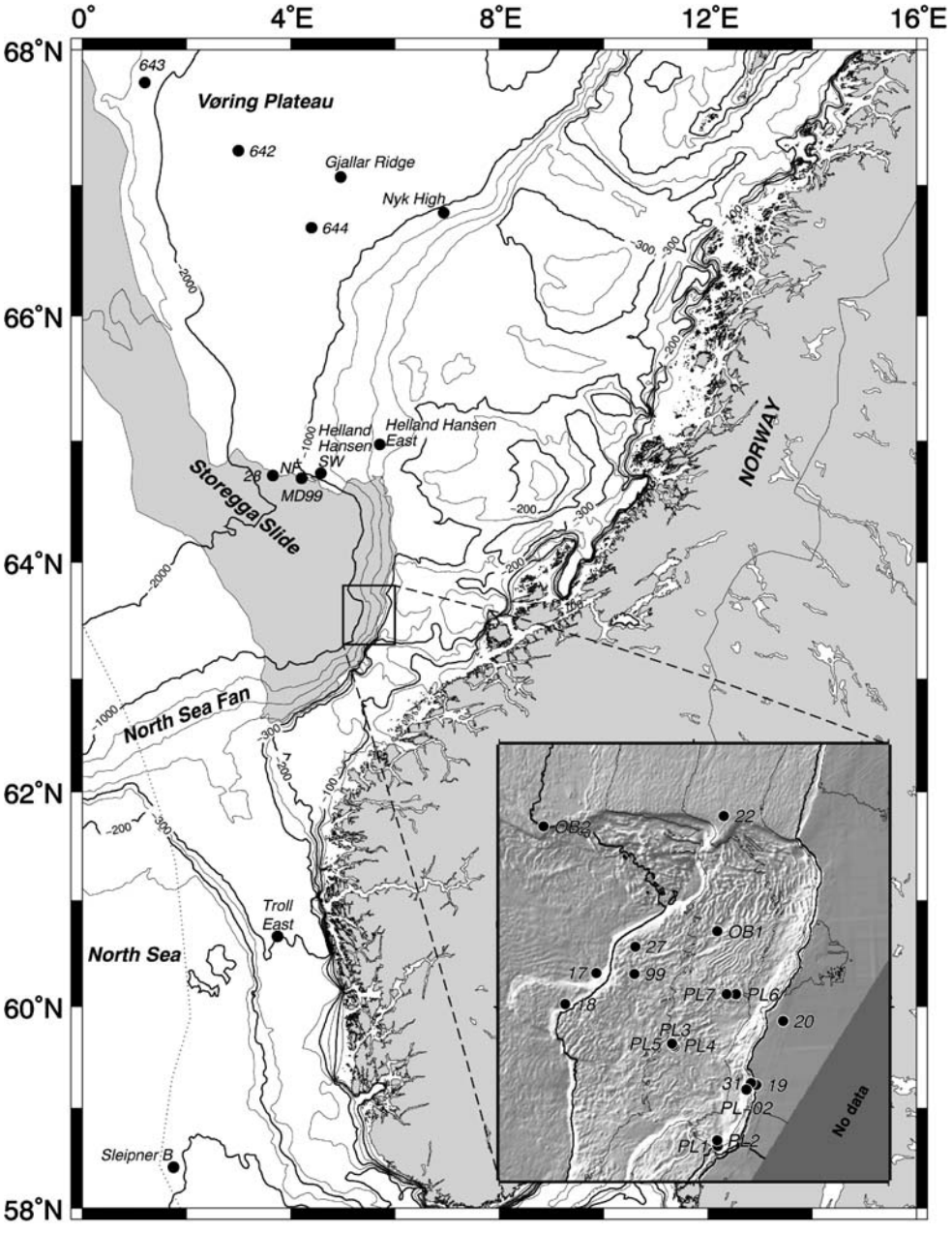

Fig. 1 Locations of the boreholes used in this study (also see Table 1). The bathymetric contour interval is 500 m. The Storegga Slide is indicated in *grey*

glacial debris flows on the slope, both comprising poorly sorted, clay-rich sediments with varying amounts of silt, sand and gravel. The much longer periods, which can be as much as 80–90% of a full glacial–interglacial cycle, during which the ice sheet retreated from the shelf edge, are characterised by fine-grained marine to distal glacial marine hemipelagic sediments. These have clay contents often exceeding 60%, and are consequently relatively poor in coarser fractions. Storegga Slide studies have shown that the main slip planes of the slide are found in the fine-grained hemipelagic units (Kvalstad et al. 2005).

The glacial sediments are characterised by generally low water content, low plasticity index and relatively low clay content whereas the marine clays have higher water content, higher plasticity index and higher clay content. The mineralogy of these marine clays has been investigated for a number of samples by Forsberg and Locat (2005). Illite is the dominant clay mineral, and chlorite, kaolinite and smectite occur in variable amounts. Biogenic oozes have been sampled below 110 m sediment depth in a borehole on the Gjallar Ridge and below 80 m sediment depth at site 28 (Fig. 1).

Materials and methods

All laboratory tests were carried out at the Norwegian Geotechnical Institute, Oslo. The various parameters included in the regression analyses were subdivided into two broad classes, these being physical parameters and mechanical parameters. The physical parameters were further subdivided into measured and derived parameters. Furthermore, a selected literature survey was conducted on earlier work dealing with two main mechanical parameters, i.e. compression index and shear strength. All parameters used in this study are described in Table 2.

Measured physical parameters

The methods used to measure water content, bulk density, density of the solid particles, grain-size distribution, and liquid and plastic limits are described in NORSOK Standard G-001 (NORSOK 2004). Natural or initial relative *water content*, W_i, is defined as the mass of water per unit mass of solid material. The *liquid* and *plastic limits* (Atterberg limits), W_p and W_l, which are the highest and lowest water content, respectively, in a plastic state, were

Table 2 Definition of sediment parameters and statistical variables

Parameters	Data	Abbreviated term, symbol	Definition	Units
Physical	Measured	W_i	Relative water content	%
		c	Clay content	%
		W_p	Plastic limit	%
		W_l	Liquid limit	Dimensionless (−)
		W_s	Shrink limit	%
		G_s	Specific density	Dimensionless (−)
	Derived	I_p	Plastic index	%
		I_l	Liquid index	Dimensionless (−)
		act (I_p/c)	Activity	Dimensionless (−)
		e_i	Void ratio	Dimensionless (−)
		e_l	Void ratio at liquid limit	Dimensionless (−)
		e_i/c	Interclay void ratio	Dimensionless (−)
Mechanical	Any type of test for undrained shear strength	*Su*	Undrained shear strength	kPa
	Fall-cone tests	Su_{FC}	Undisturbed undrained shear strength	kPa
		Su_{re}	Remoulded shear strength	kPa
		St	Sensitivity	Dimensionless (−)
	Pocket penetrometer tests	Su_{PP}	Undisturbed undrained shear strength	kPa
	Triaxial tests	Su_c	Undrained shear strength by compression tests	kPa
		Su_e	Undrained shear strength by extension tests	kPa
	Direct simple shear tests	Su_{DSS}	Undrained shear strength	kPa
	Oedometer tests	C_c	Compression index	Dimensionless (−)
Others		σ'_v	Effective overburden pressure	kPa
		P_{atm}	Atmospheric pressure	kPa

measured from remoulded samples according to NS8003 and ASTM standard (ASTM 1975; NS8003 1982).

Grain-size distributions were determined by the falling drop method for the silt (grain sizes 0.002–0.06 mm) and clay fractions (grain sizes<0.002 mm), and by dry sieving for sand (grain sizes 0.06–2 mm) and coarser material. The general character of mixed-grained soils is determined almost entirely by the smallest soil constituents (Terzaghi et al. 1996), if the content of these smallest constituents reach a certain level. Thus, the *clay content*, c, of a sediment is an important parameter.

Derived physical parameters

The *plasticity index*, I_p, shows the range of water content for which the sediment is in a plastic state. It is calculated as the difference between the liquid and plastic limits, $I_p=W_l-W_p$. The *liquid index*, I_l, is an indicator of the stiffness and the degree of compaction of an in situ clay, and is estimated as $I_l=(W_i-W_p)/(W_l-W_p)$. Another parameter derived from the Atterberg limits is *activity*, which is defined as the plasticity index divided by clay content (I_p/c).

The *void ratio*, e, of a sediment is the ratio of the volume of voids to the volume of solids and shows to which degree a sediment can be termed loose or dense. The natural or initial void ratio is calculated assuming a fully saturated sediment, $e_i=W_i\rho_s$, where ρ_s is the density of solid particles. Similarly, the *void ratio at the liquid limit* is determined as $e_l=W_l\rho_s$. A parameter found particularly useful in this study is the *interclay void ratio*, defined as the initial void ratio divided by the clay content in decimal fractions of 1.0 (e_i/c). The interclay void ratio reflects the influence of clay content alone, independently of the other grain-size fractions, and can be used to estimate the mechanical property of clay-rich sediments.

Mechanical parameters

Undisturbed and *remoulded undrained shear strength*, Su_{FC} and Su_{re}, respectively, were measured using a fall-cone apparatus. *Sensitivity*, *St*, is calculated as the undisturbed shear strength divided by the remoulded shear strength. Undrained shear strength was measured also by anisotropic compression triaxial tests (Su_c). Compressibility is an important engineering parameter, and the *compression index*, C_c, is commonly used to predict the amount of expected settlement of sediment under a given pressure. Continuous rate of strain (CRS) oedometer tests were used to determine the compression index of the samples, based on the relationship $C_c=(e_l-e)/\log(\sigma/\sigma_l)$ where e_l represents the void ratio at stress σ_l.

Table 3 Determination of compression index, based on a selected literature survey (for definition of parameters, see Table 2)

Equation type	Applicability	Reference
$C_c = a + bW_i$	All clays	Azzouz et al. (1976); Koppula (1981); Herrero (1983)
	Organic silt and clays	Bowles (1989)
	Scandinavian clays	Janbu (1985)
	Soft clays	Mesri et al. (1994)
$C_c = a + be_i$	Inorganic and organic soils	Hough (1957)
	Motley clays from Sao Paulo, lowlands of Santos, Brazil	Cozzolino (1961)
	All clays	Azzouz et al. (1976)
	Eastern Canadian clays	Leroueil et al. (1983)
	Chicago clays	Bowles (1989)
$C_c = a + bW_l$	Remoulded clays	Skempton (1944)
	Brazilian clays	Cozzolino (1961)
	Normally consolidated clays	Terzaghi and Peck (1967)
	All clays with W_l<100%	Azzouz et al. (1976)
	Natural and artificial soils	Hirata et al. (1990)
$C_c = ae_l$	Remoulded normally consolidated clays	Nagaraj and Srinivasa Murthy (1983, 1986)
	Clay–sand mixture	Nagaraj et al. (1995)
$C_c = e_i/(a + be_i)$	Ariake clay	Park and Koumoto (2004)
$C_c = ae_i^b$	Naturally sedimented young soils	Shorten (1995)
$C_c = aI_pG_s$	All remoulded, normally consolidated clays	Wroth and Wood (1978)
$C_c = a + b(W_l - W_s)$	Remoulded clays	Sridharan and Nagaraj (2000)
$C_c = a(W_l - W_p) + bI_p(c + act^{-1})$	Remoulded, normally consolidated clays	Carrier (1985)

Note that a and b (y intercept and slope in a linear regression) are soil/sediment-dependent

Table 4 Determination of shear strength, based on a literature survey (for definition of parameters, see Table 2)

Equation	Applicability	Reference
$Su/\sigma'_v = f(I_l)$	Normally consolidated clays	Bjerrum and Simons (1960)
$Su/\sigma'_v = f(I_p)$	Normally consolidated clays	Bjerrum and Simons (1960)
	Remoulded Japanese marine clays	Nakase and Kamei (1988)
	Normalized consolidated inorganic clays	Ladd (1991)
	Eastern Canadian clays	Leroueil et al. (1983)
$Su = 170\exp(-4.6I_l)$	All remoulded soils	Wroth and Wood (1978)
$Su = \exp(-3.361I_l + 0.376)$	Remoulded natural clays	Hirata et al. (1990)
$Su = \exp(-3.262I_l - 0.566)$	Remoulded artificial clays	Hirata et al. (1990)
$Su = (19.8/I_l)^{2.44}$	Su<73 kPa	Locat and Demers (1988)
$Su = 1/(I_l - 0.21)^2$	Eastern Canadian clays	Leroueil et al. (1983)
$(Su/P_{atm})^{-0.158} = 0.981 + 1.092I_l/(0.75 + 0.181act^{-1})$	Remoulded clays	Carrier and Beckman (1984)
$Su = 2(I_l)^{-2.8}$	Remoulded clays	Terzaghi et al. (1996)
$Su = 4.2(I_l)^{-1.6}$	Remoulded clays	NGI (2002)
$Su = 3.9(I_l)^{-2.0}$	Remoulded clays	NGI (2002)

Results

Literature survey of interrelationships between compression index, shear strength and other sediment/soil parameters

A selected literature survey on the compression index and shear strength of sediments and soils (Tables 3 and 4) shows that C_c has close relationships with many physical properties of clay, such as W_i, e_i, W_l, e_l, I_p and activity, whereas shear strength is more closely related to I_l, I_p and activity. However, most of these published relationships are not expressed with the predictive accuracies needed for designers to estimate safety factors in foundation design or slope stability analysis. Furthermore, it should be noted that these relationships are to a large degree site-specific. However, there are common equation types which could also be used at several sites (cf. below).

Relationships among Atterberg limits, water content and clay content

Plasticity charts are very useful for the classification of sediments (Holtz and Kovacs 1981). The A-line, I_p=0.73 (W_l−20), generally separates clay-rich sediments from silty sediments, and organic-rich sediments from inorganic sediments (Fig. 2). The U-line, I_p=0.9(W_l−8), indicates the upper boundary of expected results for natural soils.

The categories shown in Fig. 2 are: *ML&OL* inorganic and organic silts and silty clays of low plasticity, rock flour, silty or clayey fine sands, *MH&OH* micaceous or diatomaceous fine sandy and silty soils, elastic silts, organic silts, clays and silty clays, *CH* inorganic clays of high plasticity, and *CL* inorganic clays, sandy and silty clays with low to medium plasticity.

Most of the sediments in the study area classify as inorganic clays with low, medium or high plasticity. By

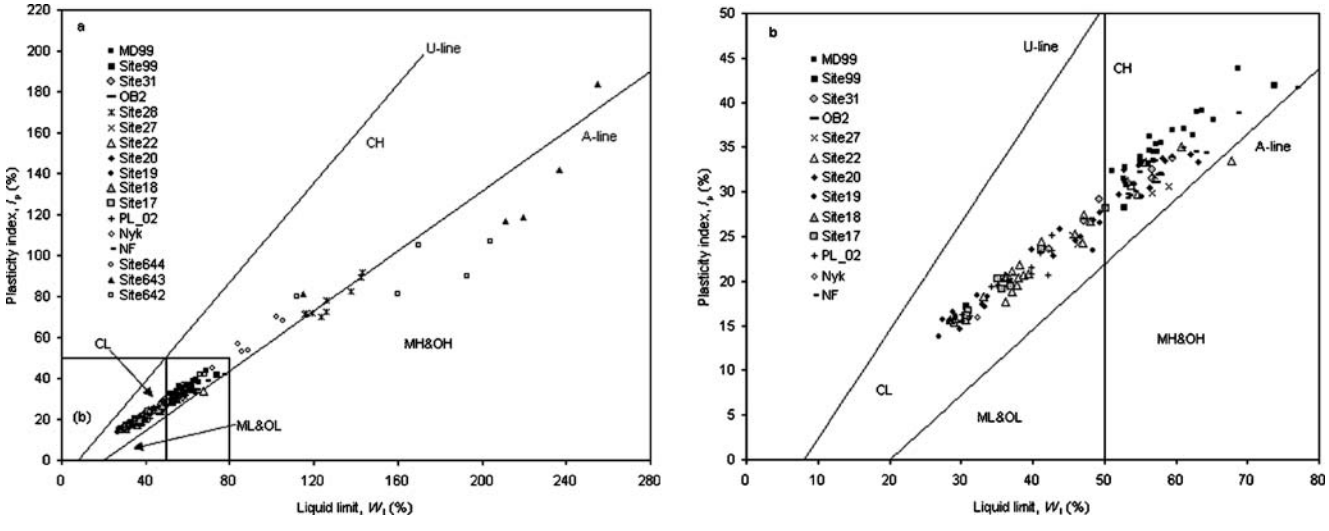

Fig. 2a, b Plasticity charts. **a** All data from the present study. **b** Enlarged plot of data inside the *rectangle* in (**a**)

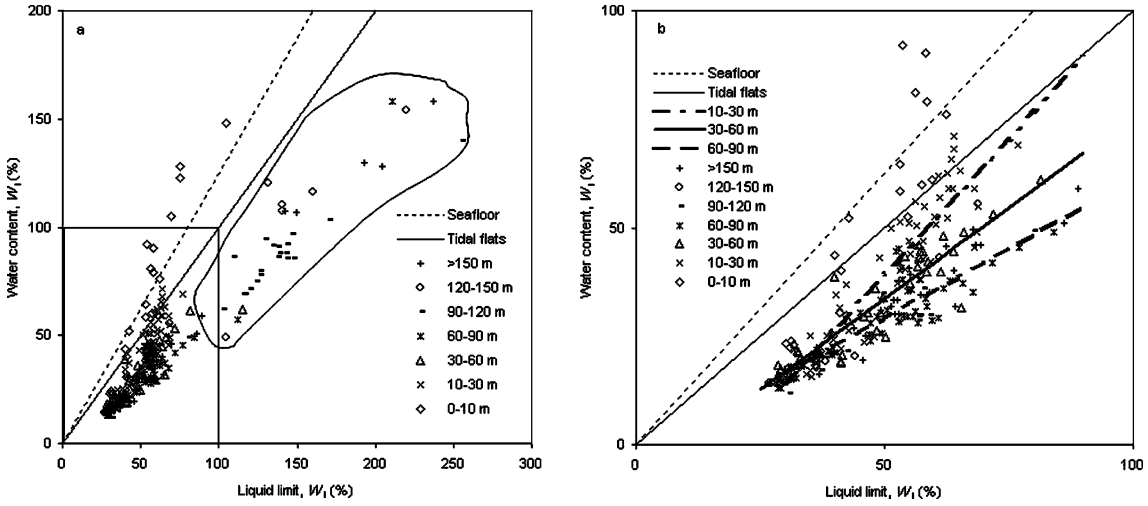

Fig. 3a, b Relative water content versus liquid limit of sediments from different depths below the seafloor. The lines *seafloor* and *tidal flats* are from Skempton (1970). **a** All data in the present study. **b** Enlarged plot of data inside the *rectangle* in (**a**)

contrast, sediments from ODP sites 643 and 642, located to the north of the Storegga Slide, plot in the region of organic clay. Ooze documented at site 28 in Storegga Slide sediments is on or below the A-line in the plasticity charts (Fig. 2a). This means that this ooze is different from most of the sediments studied in these charts.

In Fig. 3a, the relationship between the water content and liquid limit for the borehole sites in this study is compared with data from Skempton (1970), who analysed samples from the upper 25 cm at six seafloor locations and three intertidal flats at Gosport, Avonmouth and Atanpit. The values on or to the left of the seafloor line are from the top 10-m layer of the boreholes. There are four samples from sites southwest of the Helland Hansen and Gjallar Ridge which have relatively high water contents of ca. 100–150%. The liquid limits of oozes from the Storegga site 28 and the Gjallar Ridge site are high, as well as for sediments from ODP sites 642, 643 and 644 which show high water contents (cf. data points in encircled area in Fig. 3a).

In Fig. 3b, the data at depths of 10–30, 30–60 and 60–90 m were analysed by linear regression analyses, except for the highly overconsolidated samples which were not included in these assessments. The regression equations are shown in Table 5 and the regression lines plot in Fig. 3b.

Figure 4 shows that the borehole sediments studied here have clay contents varying in the range 25–70%. Most samples plot as inactive clay (cf. categories of Skempton 1953), with activities between those of kaolinite and illite. By contrast, the samples from ODP sites 643 and 642 as well as the ooze from the Storegga site 28 are active clays (Fig. 4).

Table 5 Regression equations for water content and liquid limit (see also Fig. 3b; *n* number of samples, *r* correlation coefficient)

Depth (m)	Equation	*n*	*r*
10–30	$W_i = -23.19 + 1.247 W_l$	54	0.805
30–60	$W_i = -8.22 + 0.837 W_l$	39	0.803
60–90	$W_i = -3.00 + 0.642 W_l$	45	0.778

The data presented above demonstrate that sediments from ODP sites 642, 643 and 644 and oozes from the Storegga Slide site 28 and the Gjallar Ridge site differ from those of the other sites in terms of I_p, W_l and c. Therefore, these data are not included in the following regression analyses, nor are those for four surface samples with water contents exceeding 100% at the sites southwest of the Helland Hansen and Gjallar Ridge, because these samples were too soft and not well consolidated. The highly overconsolidated samples are also not considered further in the following analyses, due to the large overburden loss caused by slide events.

Compressibility

Simple regression analyses were performed for interrelationships between C_c and W_i, W_l, I_p, e_i, e_l and e_i/c (Table 6).

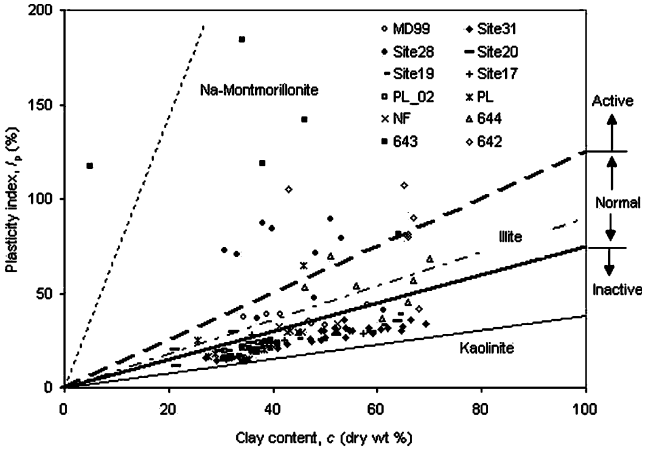

Fig. 4 Data from the present study plotted in an activity chart of clay. The boundary lines for inactive (*act*<0.75), normal (0.75<*act*<1.25) and active (*act*>1.25) clay are from Skempton (1953). The lines for montmorillonite, illite and kaolinite are from Lambe and Whitman (1969)

Table 6 Regression equations for the compression index, Storegga Slide region

Regression method	Equation	n	r
Simple	$C_c = 0.0017 + 0.0094W_i$	99	0.925
	$C_c = -0.128 + 0.0086W_l$	58	0.867
	$C_c = -0.075 + 0.013I_p$	58	0.848
	$C_c = 0.004175I_p^{1.227}$	58	0.844
	$C_c = -0.0026 + 0.336e_i$	99	0.926
	$C_c = -0.126 + 0.310e_l$	58	0.868
	$C_c = 0.141 + 0.074e_i/c$	72	0.636
Multiple	$C_c = -0.093 + 0.0061W_i + 0.0041W_l, r(W_i) = 0.739, r(W_l) = 0.605$	58	0.942
	$C_c = -0.069 + 0.0065W_i + 0.006I_p, r(W_i) = 0.767, r(I_p) = 0.592$	58	0.940
	$C_c = -0.136 + 0.103W_l - 0.0027I_p, r(W_l) = 0.345, r(I_p) = 0.061$	58	0.868
	$C_c = -0.0892 + 0.0062W_i + 0.0033W_l + 0.0012I_p, r(W_i) = 0.738, r(W_l) = 0.163, r(I_p) = 0.039$	58	0.942

Note that n is number of samples, r is correlation coefficient

Only typical plots between C_c and e_i and e_l based on these regression analyses are given in Fig. 5. The relationship between C_c and I_p was evaluated by both linear and power regressions (Fig. 5 and Table 6). The compressibility index increased more with an increase of I_p for marine clays than for glacial deposits, indicating that the relationship between C_c and I_p should be dependent on depositional processes, too. Marine sediments in the Storegga Slide area showed a plasticity index higher than 25%, and values for most of the glacial deposits were observed to be less than 25% (Kvalstad et al. 2005).

Multiple regression analyses were performed for relationships between C_c and W_i, W_l and I_p. This greatly improved the correlations, as indicated by the higher correlation coefficients (Table 6). The data were also sorted according to depth (Fig. 5), which showed no obvious

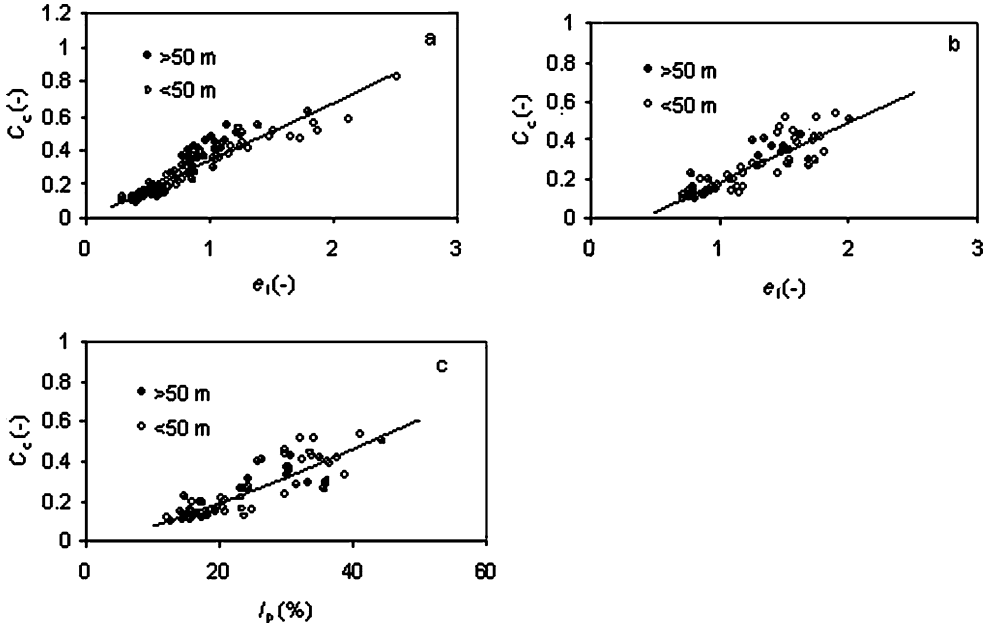

Fig. 5a–c Relationships between compression index and **a** natural void ratio, **b** void ratio at liquid limit and **c** plasticity index (see Table 5 for equations). The 50 m value is depth below seafloor

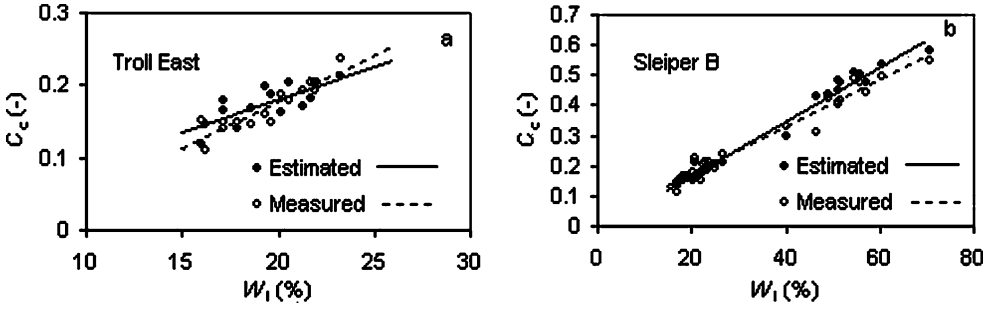

Fig. 6a, b Measured and estimated relationships between C_c and W_i, based on multiple regression analysis of data from the sites **a** Troll East and **b** Sleiper B (data from NGI 2002)

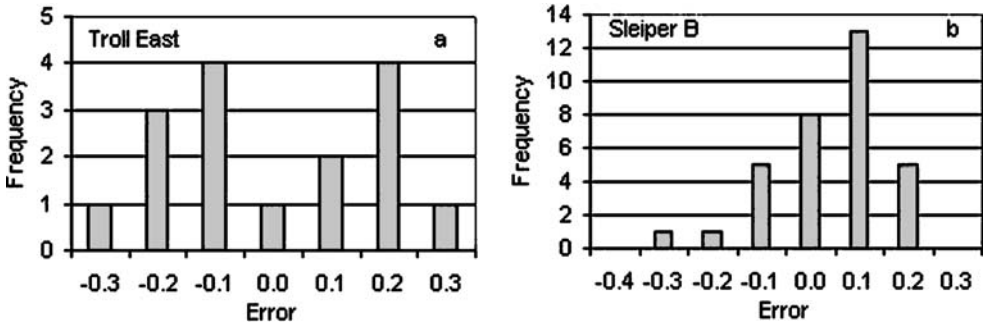

Fig. 7a, b Prediction error histograms for the compression index for data from **a** Troll East and **b** Sleiper B

trend between depth (overburden pressure) and the variables.

Data from the sites Troll East and Sleiper B (NGI 2002) were used to test if the regression equations could be used for other sites of similar geological setting. The first multiple regression equation in Table 6 was used for this purpose, and the estimated values from this equation and the measured values are shown in Fig. 6. The error is calculated as $\frac{measured\ value - estimated\ value}{measured\ value}$, the relationship between the calculated error and frequency being shown in Fig. 7. The results show that 88% of occurrence is found between error −0.2 and 0.2 for the site Troll East, and 97% of occurrence is found in the same range for the site Sleiper B (Fig. 7). This means that good fit exists.

Undrained shear strength

The SHANSEP model (Ladd and Foott 1974) was used to evaluate the undrained shear strength where the effect of overconsolidation is included. The undrained strengths from triaxial compression and extension tests and direct simple shear tests have been thoroughly evaluated. This has been presented in detail by Kvalstad et al. (2005), and will not be discussed further in this paper. Here, the undrained shear strength data are discussed only for normally consolidated samples. The plot of the stress ratio (ratio between undrained shear strength, Su_{FC}, and effective overburden pressure, σ_v') versus effective overburden pressure shows scattered data points at shallow depths with small σ_v' values (Fig. 8). The stress ratios from triaxial tests have been observed to be around 0.27 for the marine clays, and about 0.32 for the glacial deposits (Kvalstad et al. 2005).

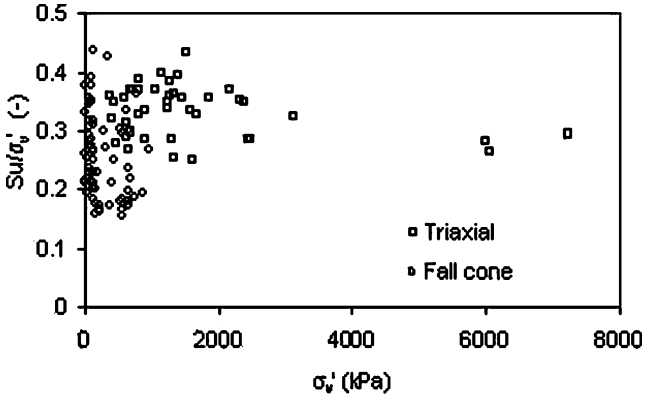

Fig. 8 Relationship between the stress ratio and effective overburden pressure

Undrained shear strengths from fall-cone and triaxial tests are analysed statistically below by considering their relationships with key physical parameters.

Fall-cone tests

In the regression analyses of undrained shear strength from fall-cone tests vs. key physical parameters, only the samples at depths less than 80 m below seafloor were

Table 7 Regression equations for shear strength, Storegga Slide region (n number of samples, r correlation coefficient)

Parameter	Equation	n	r
Su_{FC}	$Su_{FC} = 353.7 \exp(-0.0479 W_i)$	114	0.701
	$Su_{FC} = 231.9 \exp(-2.96 I_l)$	98	0.833
	$Su_{FC} = 3,172.5 \exp(-6.03 act)$	76	0.757
	$Su_{FC} = 1,397.2 \exp(-1.48 e_i/c)$	76	0.880
	$Su_{FC} = 7,603.8 (W_i)^{-1.35}$	114	0.709
	$Su_{FC} = 16.13 (act)^{-3.21}$	76	0.748
	$Su_{FC} = 53.1 (I_l)^{-0.35}$	98	0.711
	$Su_{FC} = 382.8 (e_i/c)^{-2.39}$	76	0.880
Su_{re}	$Su_{re} = 357.3 \exp(-0.071 W_i)$	114	0.748
	$Su_{re} = 3,073.7 \exp(-7.16 act)$	78	0.804
	$Su_{re} = 159.6 \exp(-3.97 I_l)$	102	0.813
	$Su_{re} = 2,037.2 \exp(-2.10 e_i/c)$	78	0.870
	$Su_{re} = 16,733.0 (W_i)^{-1.78}$	114	0.743
	$Su_{re} = 7.134 (act)^{-3.47}$	78	0.793
	$Su_{re} = 27.37 (I_l)^{-0.39}$	102	0.659
	$Su_{re} = 296.5 (e_i/c)^{-3.13}$	78	0.865
St	$St = 0.477 + 0.062 W_i$	98	0.811
	$St = 1.434 + 2.810 I_l$	98	0.783
	$St = -0.706 + 5.381 act$	76	0.647
	$St = 0.445 + 0.987 e_i/c$	76	0.812
Su_{PP}–Su_{FC}	$Su_{FC} = 14.28 + 0.842 Su_{pp}$	68	0.947
Su_c	$Su_c = 818.3 \exp(-4.17 I_l)$	91	0.775
	$Su_c = 2,235.5 \exp(-1.22 e_i/c)$	37	0.712

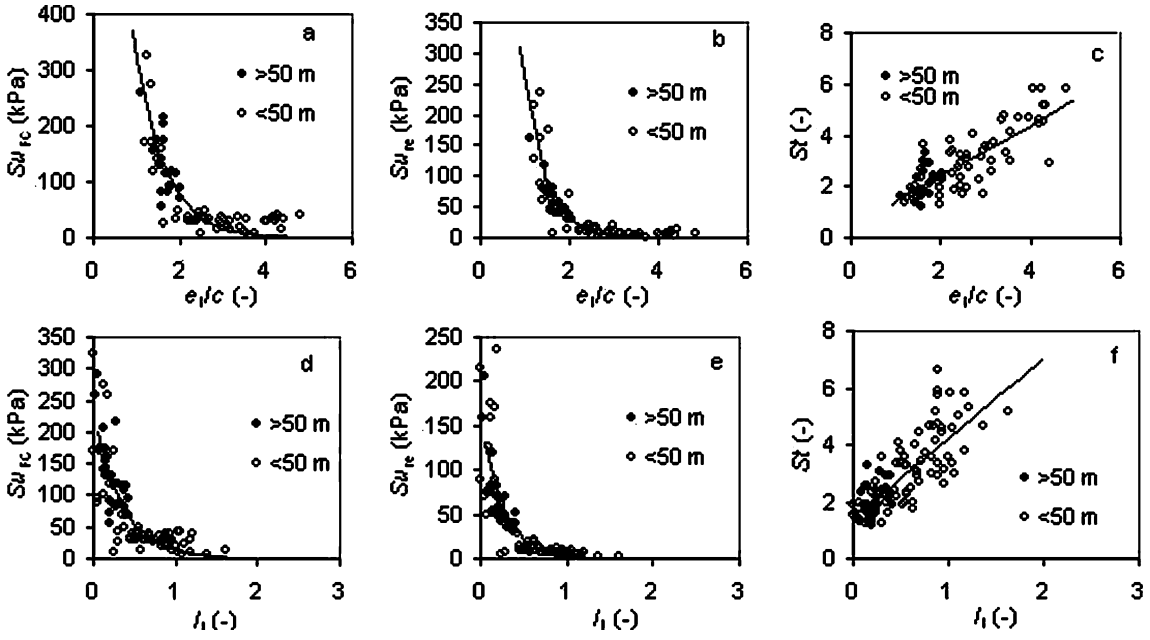

Fig. 9a–f Relationships between the undisturbed undrained shear strength, remoulded shear strength, sensitivity and key physical parameters: **a**–**c** interclay void ratio and **d**–**f** liquidity index. The 50 m value is depth below seafloor

investigated. The reason for this is the high likelihood of sample swelling at greater depths (NGI 2001).

The best-fit regression equations (Table 7) are of the types $y=ae^{(bx)}$ and $y=a(x)^b$. In the present case, the former regression type was associated with a higher correlation coefficient. From these analyses, the interclay void ratio, e_i/c, seems to show the best relationship with shear strength. Sensitivity shows a linear relationship with the physical parameters investigated, the corresponding regression equations being given as reference in Table 7. Only typical regression plots between undrained shear strength (undisturbed and remoulded), sensitivity and key physical parameters (interclay void ratio and liquidity index) are presented in Fig. 9. Results from the site Troll East (Fig. 10) show that the regression equations in this study can be used in estimating undisturbed and remoulded shear strength also for other sites, but that data from the site Troll East are more scattered at low interclay void ratios than at higher values. Most of the error prediction is conservative (Fig. 11).

The data points in Fig. 9 are sorted by depths greater or less than 50 m. The general trend shows that undrained shear strength is related to overburden pressure. At depths exceeding 50 m, the water content, interclay void ratio and liquid limit are lower.

Multiple regression analyses were also performed to assess relationships between shear strength and key physical parameters, but goodness of fit was not measurably improved (data not given in Table 7).

Pocket penetrometer tests

Measurements of undrained shear strength are commonly known to be influenced by the method used. In the samples used for this study, however, there is a good relationship

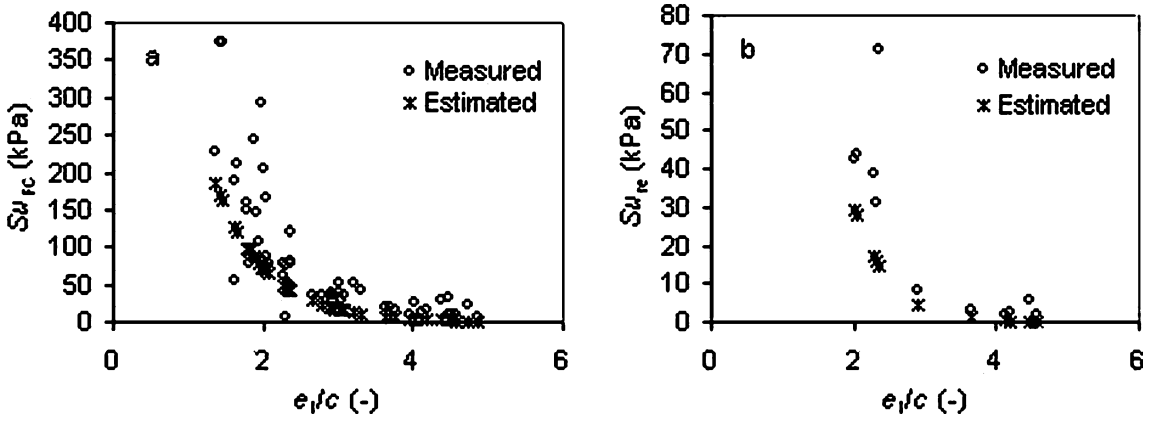

Fig. 10a, b Relationships of measured and estimated undisturbed (**a**) and remoulded (**b**) shear strength versus interclay void ratio for the site Troll East (data from NGI 2002)

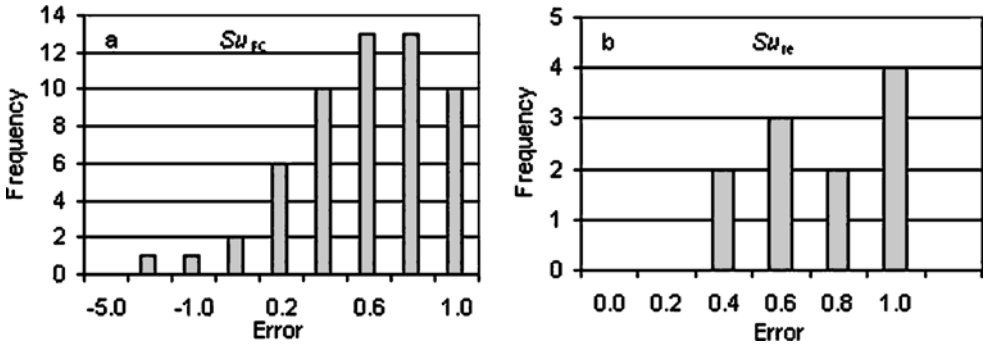

Fig. 11a, b Predicted error histograms for intact (**a**) and remoulded (**b**) shear strength for the site Troll East

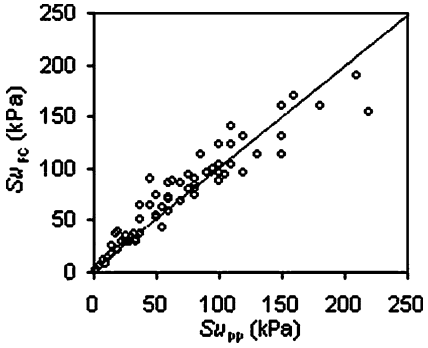

Fig. 12 Comparison between undrained shear strengths measured with a fall-cone apparatus (*FC*) and a pocket penetrometer (*PP*). The data are for depths less than 80 m below seafloor

between the undisturbed shear strength values from fall-cone measurements and from the pocket penetrometer (Fig. 12). Only data at depths less than 80 m are shown in Fig. 12, due to possible sample swelling at greater depths.

Triaxial and direct simple shear tests

Relationships between the undrained shear strength from triaxial compression tests (Su_c) for normally consolidated soils, the interclay void ratio (Fig. 13a) and the liquidity index (Fig. 13b) were investigated by simple regression analyses (Table 7). The data are sorted by depth in order to evaluate any influence of overburden pressure on undrained shear strength.

Undrained shear strengths measured by means of the triaxial extension test (Su_e) and the direct simple shear (DSS) test (Su_{DSS}) have also been carried out for sediments of the Storegga Slide area, strength anisotropy having been evaluated by Kvalstad et al. (2005) as Su_{DSS}/Su_c=0.8 and Su_e/Su_c=0.7. The estimated shear strengths for these two loading modes, using the above formula, are also given in Fig. 14. The undrained shear strengths from triaxial tests or DSS tests show higher values than those from fall-cone tests or pocket penetrometer tests, at a given interclay void ratio (Fig. 14a) or liquidity index (Fig. 14b). The values measured from fall-cone tests (cf. bottom curve in Fig. 14) and triaxial compression tests (cf. top curve in Fig. 14) can be considered as the low and high boundaries, respectively, for the strength parameters.

Discussion and conclusions

The analyses of various physical properties, compression and strength parameters of sediments in the Storegga Slide region provide a unique opportunity to establish robust parameter interrelationships and to evaluate geotechnical behaviour based on a large dataset derived from boreholes. Since the geological setting and depositional patterns on the Mid-Norwegian continental margin are quite typical for glaciated continental margins (Solheim et al. 1998; Nielsen et al. 2005), we consider the relationships established in this study relevant also for other regions with similar geological settings. Indeed, there are universal relationships between such parameters even for various geographic environments (Flemming and Delafontaine 2000). The equation types in the present study are universal for both sediments in marine environments and soil deposited from

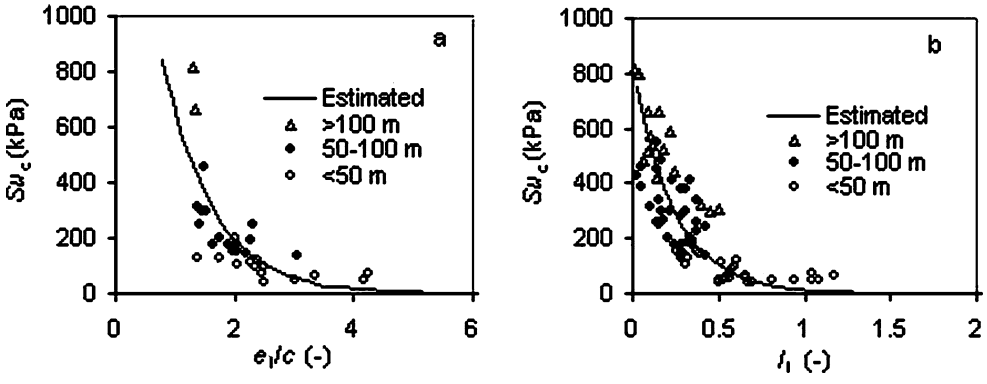

Fig. 13a, b Relationships between undrained shear strength measured by triaxial compression tests and **a** interclay void ratio and **b** liquidity index. Note that the data are differentiated based on depths below seafloor

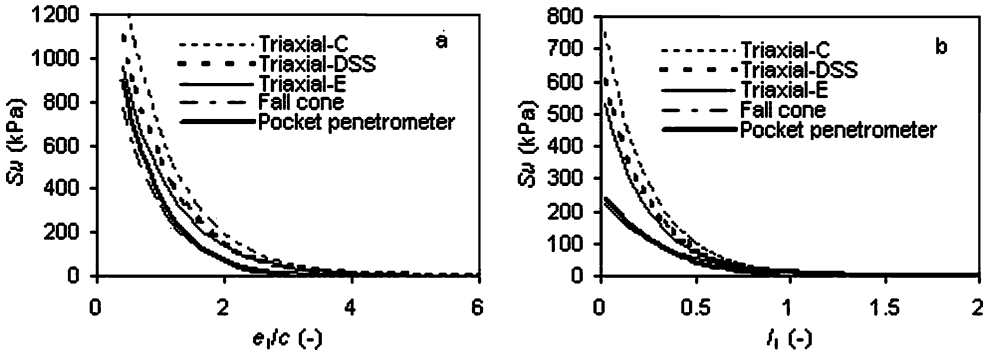

Fig. 14a, b Relationships of estimated undrained shear strengths based on triaxial extension and direct simple shear tests, measured undrained shear strengths based on triaxial compression tests, and fall-cone and pocket penetrometer tests versus **a** the interclay void ratio and **b** the liquidity index

terrigenous environments. However, the y intercept and slope in the linear regressions should be considered as site-specific.

In the W_i versus W_l plot (Fig. 3), most borehole data points are located below the tidal flat line of Skempton (1970). For the depth intervals 10–30, 30–60 and 60–90 m below seafloor, the slopes of the regressions decrease progressively with increasing depth values. This trend demonstrates the influence of overburden pressure on the relationship between W_i and W_l.

Because compressibility depends mainly on clay content and the mineral components of sediments, no obvious trend between depth (overburden pressure) and the variables can be observed in Fig. 5.

The regression analyses show that the sediments have high compressibility and low strength when the water content and clay content are high. In the study area, the glacial deposits with low water content and low clay content showed low compressibility and high strength. The marine sediments, on the other hand, deposited during interglacial or interstadial periods, are fine-grained with higher water content and higher clay content. These marine deposits show high compressibility and low strength as well as high sensitivity, consistent with these units forming the slip planes or failure zones for submarine sliding in this area.

Some distinct limitations of this parameter study should be pointed out. Samples from great depths tend to swell after recovery to the surface. The undrained shear strengths measured with simple devices such as a fall cone or a pocket penetrometer at greater depths (more than 80 m below seafloor) should be used with care due to the possible disturbance of the samples. The relationships between the water content and compression index should also be used with care in such cases. In this study, organic material deposited at ODP sites and ooze at the Storegga Slide site were not included in the regression analysis. Further study is needed to obtain relationships between the mechanical and physical parameters for these materials.

Based on the data presented above, the following conclusions are drawn.

- Most of the sediments in the study area classify as inactive and normal clay. The plasticity is variable, from low to high.
- Relationships between physical and mechanical parameters are marked.
- Multiple regression analyses between the compression index and physical parameters yield better results than do simple regression analyses. The simple regression equation between the undrained shear strength and interclay void ratio shown is the best fit for the estimation of undrained shear strength for the region.
- Relationships between key physical and mechanical properties, based on regression analyses, can be used to estimate the compression index and undrained shear strength of sediments.
- Fine-grained marine sediments of the Storegga Slide region show high water content, low strength and high compressibility. This supports these marine layers being the sliding planes for the Storegga Slide.

Acknowledgement This is publication number 112 of the International Centre for Geohazards (ICG), and was prepared within the framework of the Euromargin project (European Science Foundation 01-LEC-EMA14F).

References

ASTM (1975) ASTM Standard D2487. Standard test method for classification of soils for engineering purposes. American Society for Testing and Materials, West Conshohocken, Pennsylvania

Azzouz AS, Krizek RJ, Corotis RB (1976) Regression analysis of soil compressibility. Soils Foundations 16(2):19–29

Berg K, Solheim A, Bryn P (2005) The Pleistocene to recent geological development of the Ormen Lange area. Mar Petrol Geol 22:45–56

Bjerrum L, Simons NE (1960) Comparison of shear strength characteristics of normally consolidated clays. In: Proc ASCE Res Conf shear strength of cohesive soils. Boulder, Colorado, pp 711–726

Bowles JE (1989) Physical and geotechnical properties of soils. McGraw-Hill, New York

Carrier WD III (1985) Consolidation parameters derived from index tests. Geotechnique 35(2):211–213

Carrier WD, Beckman JF (1984) Correlations between index tests and the properties of remoulded clays. Geotechnique 34 (2):211–228

Cozzolino VM (1961) Statistical forecasting of compression index. In: Proc 5th int conf soil mechanics and foundation engineering, vol 1. Presses Universitaires de France, Paris, pp 51–53

Eldholm O, Thiede J, Taylor E (1987) ODP proceedings of the initial reports A 104. College Station, Texas

Flemming BW, Delafontaine MT (2000) Mass physical properties of muddy intertidal sediments: some applications, misapplications and non-applications. Cont Shelf Res 20:1179–1197
Forsberg CF, Locat J (2005) The evolution of the Storegga region, offshore Norway as seen from mineralogical and microfabric analyses. Mar Petrol Geol 22:109–122
Haflidason H, Sejrup HP, Nygård A, Mienert J, Bryn P et al. (2004) The Storegga Slide: architecture, geometry and slide development. Mar Geol 213:201–234
Haflidason H, Lien R, Sejrup HP, Forsberg CF, Bryn P (2005) The dating and morphometry of the Storegga Slide. Mar Petrol Geol 22:123–136
Herrero OR (1983) Universal compression index equation; closure. Geotech Eng ASCE 109(5):755–761
Hirata S, Yao S, Nishida K (1990) Multiple regression analysis between the mechanical and physical properties of cohesive soils. Soils Foundations 130(3):91–108
Holtz RD, Kovacs WD (1981) An introduction to geotechnical engineering. Prentice-Hall, Englewood Cliffs, New Jersey
Hough BK (1957) Basic soils engineering, 1st edn. Ronald, New York
Janbu N (1985) Soil models in offshore engineering. Geotechnique 35(3):241–281
Koppula SD (1981) Statistical estimation of compression index. Geotech Testing 4(2):68–73
Kvalstad TJ, Nadim F, Kaynia AM, Mokkelbost KH, Bryn P (2005) Soil conditions and slope stability in the Ormen Lange area. Mar Petrol Geol 22:299–310
Ladd CC (1991) Stability evaluation during stage construction. Geotech Eng ASCE 117(4):540–615
Ladd CC, Foott R (1974) New design procedures for stability of soft clays. Proc ASCE GT7:763–786
Lambe TW, Whitman RV (1969) Soil mechanics. Wiley, New York
Leroueil S, Tavenas F, Lebihan JP (1983) Propriétés caractéristiques des argyles de l'est du Canada. Can Geotech J 20(4):681–705
Locat J, Demers D (1988) Viscosity, yield stress, remoulded strength and liquidity index relationships for sensitive clays. Can Geotech J 25:799–806
Mesri G, Kwan Lo DO, Feng TW (1994) Settlement of embankments on soft clays. Vertical and horizontal deformations of foundations and embankments. ASCE Geotech Spec Publ 40 (1):8–56
Mienert J (2004) COSTA continental slope stability: major aims and topics. Mar Geol 213:1–7
Mienert J, Berndt C, Laberg JS, Vorren TO (2003) Submarine landslides on continental margins. In: Wefer G, Billett D, Hebbeln D, Jørgensen BB, Schlüter M, Veering TCE van (eds) Ocean margin systems. Springer, Berlin Heidelberg New York, pp 179–193
Nagaraj TS, Srinivasa Murthy BR (1983) Rationalization of Skempton's compressibility equation. Geotechnique 33 (40):433–443
Nagaraj TS, Srinivasa Murthy BR (1986) A critical reappraisal of compression index equations. Geotechnique 36(1):27–32
Nagaraj TS, Pandian NS, Narasimha Raju PSR, Vishnu Bhushan T (1995) Stress–state–time-permeability relationships for saturated soils. In: Proc int symp compression and consolidation of clayey soils, 10–12 May 1995, IS Hiroshima, Japan, pp 537–542
Nakase A, Kamei T (1988) Undrained shear strength of remoulded marine clays. Soils Foundations 28(1):29–40
NGI (2001) Ormen Lange site investigation 2000. Norwegian Geotechnical Institute, Oslo, Geotech Geol Rep 20001147-2
NGI (2002) Early soil investigations for "Fast track projects". Norwegian Geotechnical Institute, Oslo, Rep 521553
Nielsen T, De Santis L, Dahlgren KIT, Kuijpers A, Laberg JS et al. (2005) A comparison of the NW European glaciated margin with other glaciated margins. Mar Petrol Geol 22:1149–1183
NORSOK (2004) NORSOK Standard G-001. Standards Norway
NS8003 (1982) Norwegian standard. Geotechnical testing. Laboratory methods. Fall cone liquid limit, 1st edn. Norwegian Geotechnical Institute, Oslo
Park JH, Koumoto T (2004) New compression index equation. Geotech Geoenviron Eng 130(2):223–226
Shorten GG (1995) Quasi-overconsolidation and creep phenomena in shallow marine and estuarine organo-calcareous silts, Fiji. Can Geotech J 32:89–105
Skempton AW (1944) Notes on compressibility of clays. Q J Geol Soc Lond 100(2):119–135
Skempton AW (1953) The colloidal "activity" of clays. In: Proc 3rd int conf soil mechanics, vol 1. Zurich, pp 57–61
Skempton AW (1970) The consolidation of clays by gravitational compaction. Q J Geol Soc Lond 125:373–412
Solheim A, Faleide JI, Andersen ES, Elverhøib A, Forsberg CF et al. (1998) Late Cenozoic seismic stratigraphy and glacial geological development of the East Greenland and Svalbard-Barents Sea continental margins. Q Sci Rev 17:155–184
Solheim A, Berg K, Forsberg CF, Bryn P (2005) The Storegga Slide complex: repetitive large scale sliding with similar cause and development. Mar Petrol Geol 22 (1/2):1–10
Sridharan A, Nagaraj HB (2000) Compressibility behaviour of remoulded fine grained soils and correlation with index properties. Can Geotech J 37(3):712–722
Terzaghi K, Peck RB (1967) Soil mechanics in engineering practice, 2nd edn. Wiley, New York
Terzaghi K, Peck RB, Mesri G (1996) Soil mechanics in engineering practice, 3rd edn. Wiley, New York
Wroth CP, Wood DM (1978) The correlation of index properties with some basic engineering properties of soils. Can Geotech J 15:137–145